

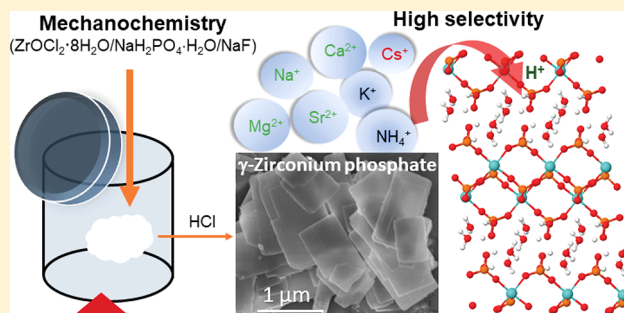
## Mechanochemistry-Based Synthesis of Highly Crystalline $\gamma$ -Zirconium Phosphate for Selective Ion Exchange

 Yu Cheng,<sup>‡</sup> Xiao Dong (Tony) Wang,<sup>§</sup> Stephan Jaenicke,<sup>‡</sup> and Gaik-Khuan Chuah<sup>\*,‡,§</sup>
<sup>‡</sup>Department of Chemistry, National University of Singapore, 3 Science Drive 3, Singapore 117543

<sup>§</sup>Bruker Singapore, 11 Biopolis Way, #10-10, Helios, Singapore 138667

### Supporting Information

**ABSTRACT:** Highly crystalline  $\gamma$ -zirconium phosphate has been synthesized by a novel minimalistic approach and investigated as a selective ion exchanger for cesium, ammonium and potassium. In contrast to current solution-based preparations, the mechanochemistry-based synthesis provides easy access to  $\gamma$ -zirconium phosphate with short synthesis times and low crystallization temperature. The addition of NaF as a mineralizer increases the crystallinity of  $\gamma$ -zirconium phosphate, which forms micrometer-sized uniformly shaped rectangular platelets. The crystalline material has extremely high selectivity to cesium even in the presence of 1000- or 500-fold excess  $\text{Na}^+$  or  $\text{Ca}^{2+}$ , respectively. The removal efficiency was >98% in the pH range of 2–5.5. As an ion exchanger for purification of dialysate, crystalline  $\gamma$ -zirconium phosphate shows higher uptake of ammonium and potassium ions than the amorphous gel compound currently used in sorbent cartridges. This sustainable protocol opens up opportunities for many practical applications of  $\gamma$ -zirconium phosphate.



## 1. INTRODUCTION

Zirconium phosphates have been investigated for applications as ion exchangers,<sup>1–3</sup> catalysts,<sup>4–7</sup> in drug delivery systems,<sup>8–10</sup> fuel cells,<sup>11–13</sup> nanocomposites,<sup>14–16</sup> and for hydrogen storage.<sup>17</sup> Zirconium phosphates are stable to high temperatures, ionizing radiation and acidic conditions. These properties make them uniquely suitable for applications in the recovery and separation of radioisotopes and treatment of radioactive wastewater. The cation exchange capacity of zirconium phosphate is also utilized in sorbent systems for dialysis.<sup>18</sup> Zirconium phosphates exist in the amorphous as well as various crystalline forms including  $\text{Zr}(\text{HPO}_4)_2 \cdot \text{H}_2\text{O}$  ( $\alpha$ -ZrP),<sup>19,20</sup>  $\text{Zr}(\text{HPO}_4)_2 \cdot 8\text{H}_2\text{O}$  ( $\theta$ -ZrP),<sup>21</sup>  $\text{Zr}(\text{PO}_4)(\text{H}_2\text{PO}_4) \cdot 2\text{H}_2\text{O}$  ( $\gamma$ -ZrP),<sup>22,23</sup> and  $\tau$ -ZrP.<sup>24</sup> Unlike the crystalline zirconium phosphates, the amorphous gel is easily prepared from precipitation of zirconium salts and phosphoric acid or phosphate salts. However, for reproducible performance, the crystalline form is highly preferred. In particular, the positioning of the phosphate groups in the crystal lattice depends on the degree of crystallinity.<sup>1</sup> With lower crystallinity, more phosphate groups are irregularly positioned in the crystal lattice resulting in cavities with a range of sizes, in contrast to the uniform cavities of the crystalline compound.<sup>25</sup> Characterization of the amorphous gel is difficult as changes resulting from small variations in the starting materials or in the synthesis may remain undetected. Crystalline zirconium phosphates are also less prone to hydrolysis than the amorphous gel, permitting us to apply the material in strongly acidic as well as fairly alkaline solutions.

The synthesis of  $\alpha$ -zirconium phosphate ( $\alpha$ -ZrP), a monohydrate with formula  $\alpha\text{-Zr}(\text{HPO}_4)_2 \cdot \text{H}_2\text{O}$ , was first reported by Clearfield and Stynes in 1964.<sup>19</sup> The crystalline compound was obtained by refluxing the amorphous zirconium phosphate gel in excess phosphoric acid. In  $\alpha$ -ZrP, coplanar zirconium atoms are sandwiched between two layers of monohydrogen phosphate groups (Figure 1a).<sup>20</sup> Within the  $\text{HPO}_4^-$ , three of the oxygen atoms are coordinated to zirconium whereas the fourth oxygen, which bears a hydrogen, points toward the interlayer space. The spacing between the layers is 7.6 Å and access to the microporous cavities is limited by the maximum opening of 2.62 Å between Zr–O from two adjacent layers.<sup>26</sup> This is adequate for unhydrated lithium, sodium and potassium ions but to accommodate the larger cesium or rubidium ions, the interlayer distance must first be enlarged by addition of a base to neutralize the lattice protons.<sup>27</sup>

Subsequently, two additional crystalline phases, the anhydrous  $\beta$ - and dihydrate  $\gamma$ -zirconium phosphate, were synthesized. Differing in the water content, they are easily interconvertible under mild conditions of controlled humidity at room temperature.<sup>22</sup> Unlike  $\alpha$ -ZrP,  $\gamma$ -ZrP does not contain any  $\text{HPO}_4^-$  groups but rather, phosphates ( $\text{PO}_4^{3-}$ ) and dihydrogen phosphates ( $\text{H}_2\text{PO}_4^-$ ). Hence, it is expressed as  $\text{Zr}(\text{PO}_4)(\text{H}_2\text{PO}_4) \cdot 2\text{H}_2\text{O}$ . The presence of these groups has been confirmed by <sup>31</sup>P MAS NMR studies where two

Received: December 23, 2017

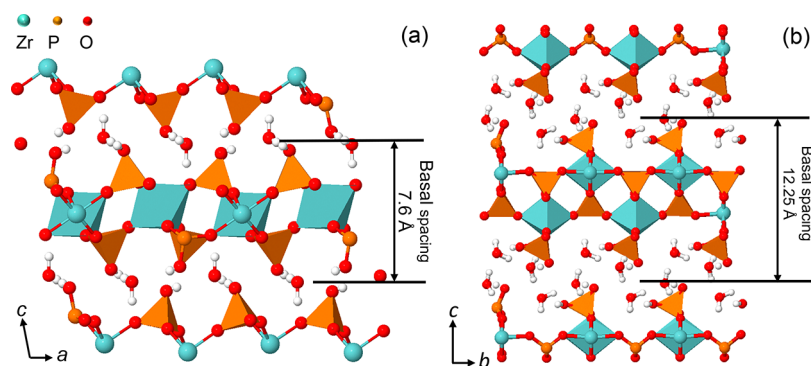


Figure 1. Structures of (a)  $\alpha$ -ZrP and (b)  $\gamma$ -ZrP.

Table 1. Reported Procedures to Form  $\gamma$ -ZrP and  $\gamma$ -NH<sub>4</sub>ZrP

	solution	method	P/Zr	F/Zr	ref
1	1 M ZrOCl <sub>2</sub> ·8H <sub>2</sub> O (0.1 mol) added to refluxing 10 M NaH <sub>2</sub> PO <sub>4</sub> ·H <sub>2</sub> O (2 mol) in 3 M HCl	refluxed for 25 h	20		22
2	1 M ZrOCl <sub>2</sub> ·8H <sub>2</sub> O (0.715 mol) added to boiling solution of 6 M NaH <sub>2</sub> PO <sub>4</sub> (14 mol) in 2 M H <sub>3</sub> PO <sub>4</sub>	refluxed for 6 weeks	27.4		34
3	1 M ZrOCl <sub>2</sub> ·8H <sub>2</sub> O (0.24 mol) added to refluxing solution of 10 M NaH <sub>2</sub> PO <sub>4</sub> (4.91 mol) in 3 M H <sub>3</sub> PO <sub>4</sub> (1.58 mol)	refluxed for 72 h, then hydrothermal treatment at 190 °C for 120 h	27.5		23
4	1 M ZrOCl <sub>2</sub> ·8H <sub>2</sub> O (0.1 mol) added to boiling 6 M NaH <sub>2</sub> PO <sub>4</sub> ·2H <sub>2</sub> O, pH adjusted to 2 using conc. HCl	sealed in Pyrex glass tubes, heated in autoclave at 190 °C for 1 week	12		36
5	2 M NH <sub>4</sub> H <sub>2</sub> PO <sub>4</sub> (0.9 mol) mixed with aqueous solution of 1.3 M ZrOCl <sub>2</sub> ·8H <sub>2</sub> O (0.065 mol) and 8 M HF	heated on a water bath at 80 °C for 5 days	13.8	6.15	30
6	7.4 M NH <sub>4</sub> F (0.3 mol) solution added to 0.5 M ZrOCl <sub>2</sub> ·8H <sub>2</sub> O (0.03 mol), pH adjusted to 2 with 2 N HCl followed by addition of 85% H <sub>3</sub> PO <sub>4</sub>	heated at 60 °C for 7 days	2	10	29
7	5 mmol ZrOCl <sub>2</sub> ·8H <sub>2</sub> O, 42–84 mmol NaH <sub>2</sub> PO <sub>4</sub> in 5 cm <sup>3</sup> H <sub>2</sub> O	sealed tube in autoclave at 250 °C for 96 h	8.3–16.7		37
8	5 mmol ZrOCl <sub>2</sub> ·8H <sub>2</sub> O, 20–83 mmol NH <sub>4</sub> H <sub>2</sub> PO <sub>4</sub> in 5 cm <sup>3</sup> H <sub>2</sub> O	sealed tube in autoclave at 250 °C for 96 h	16.7		37
9	50 mmol ZrOCl <sub>2</sub> ·8H <sub>2</sub> O, 400 mmol NH <sub>4</sub> H <sub>2</sub> PO <sub>4</sub> in 100 cm <sup>3</sup> H <sub>2</sub> O	autoclaved at 150–160 °C for 18–54 h	8		37

resonances at  $-27.4$  and  $-9.4$  ppm could be observed.<sup>28</sup> The zirconium atom is octahedrally coordinated to four oxygen atoms of the PO<sub>4</sub><sup>3-</sup> and two oxygens of the H<sub>2</sub>PO<sub>4</sub><sup>-</sup> groups (Figure 1b).<sup>23,29,30</sup> The remaining two oxygen atoms of H<sub>2</sub>PO<sub>4</sub><sup>-</sup> are bound to hydrogen atoms and project into the interlayer space where they interact with the water molecules through hydrogen bonding. The basal spacing in  $\gamma$ -ZrP is 12.25 Å, and subtracting an average layer thickness of 9.3 Å leaves an interlayer space of 2.95 Å.<sup>31</sup> Because of the larger interlayer space compared to  $\sim 1$  Å for  $\alpha$ -ZrP,<sup>10</sup>  $\gamma$ -ZrP can sorb larger ions and also has faster ion exchange rates.<sup>32–35</sup>

Despite these advantages,  $\gamma$ -ZrP has been much less studied than  $\alpha$ -ZrP. This is largely due to the difficulties in obtaining highly crystalline  $\gamma$ -ZrP. Table 1 lists the methods that have been reported for forming crystalline  $\gamma$ -phase zirconium phosphate.<sup>22,23,29,30,34,36,37</sup> Solutions containing ZrOCl<sub>2</sub>·8H<sub>2</sub>O and MH<sub>2</sub>PO<sub>4</sub> (M represents NH<sub>4</sub>, Na, or K) are refluxed or hydrothermally treated for days to weeks to achieve crystallinity. An excess of MH<sub>2</sub>PO<sub>4</sub> and additives, HF or NH<sub>4</sub>F, are typically used. This leads to large amounts of wastes that require proper treatment and disposal. In an attempt to develop an industrial method, Kobayashi conducted the synthesis in an autoclave to enable higher temperatures so that the reaction time could be shortened (Table 1, entry 9).<sup>37</sup> Despite using a Hastelloy-B autoclave, the synthesis could only be carried out at 150 °C as corrosion of the steel occurred at higher temperatures. Hence, the energy and material costs in synthesizing  $\gamma$ -ZrP is high.

We have recently synthesized highly crystalline  $\alpha$ -ZrP with variable morphologies by adopting a minimalistic approach. The reactants, ZrOCl<sub>2</sub>·8H<sub>2</sub>O and 85% H<sub>3</sub>PO<sub>4</sub>, were used in

stoichiometric amounts or with slight excess in their normal state without the use of solvents.<sup>38</sup> This “dry” green protocol was easily scalable and gave >90% yields of highly crystalline  $\alpha$ -ZrP with new morphologies and controllable particle sizes. In view of the useful properties of  $\gamma$ -ZrP, we were interested if the minimalistic protocol can be applied for its synthesis. We found that unlike  $\alpha$ -ZrP, the synthesis of  $\gamma$ -ZrP cannot be directly synthesized using H<sub>3</sub>PO<sub>4</sub> but requires sodium or ammonium dihydrogen phosphates. Therefore, an additional step is required to exchange the cation against H<sup>+</sup>. This work reports on the synthesis parameters necessary to make highly crystalline  $\gamma$ -ZrP and a study into its ion-exchange properties.

## 2. EXPERIMENTAL SECTION

**2.1. Chemicals.** Zirconium(IV) oxide chloride octahydrate (AR grade), sodium fluoride (AR grade) and strontium nitrate (>99%) were supplied by Merck. Orthophosphoric acid (85 wt %), sodium dihydrogen phosphate monohydrate, ammonium dihydrogen phosphate, cesium chloride (99.9%), ammonium nitrate (>99.5), and magnesium nitrate hexahydrate (99%) were purchased from Sigma-Aldrich. Potassium chloride (extra pure) and sodium chloride (extra pure) were obtained from GCE Laboratory Chemicals. Calcium chloride dihydrate (>99%) was from Riedel-deHaen. These chemicals were used as received.

**2.2. Synthesis.** In a typical synthesis, ZrOCl<sub>2</sub>·8H<sub>2</sub>O (3.3 mmol),  $x$ NaH<sub>2</sub>PO<sub>4</sub>·H<sub>2</sub>O ( $x = 2-5$ ) and  $y$ NaF ( $y = 0, 0.3$ ) were placed in an agate mortar and ground for  $\sim 15$  min before transferring to a 30 cm<sup>3</sup> polypropylene container. The addition of NaF was found to form highly crystalline  $\alpha$ -ZrP,<sup>38</sup> hence, its effect on the synthesis of  $\gamma$ -ZrP was investigated. The mixture was transferred into a polypropylene container and heated at 120 °C for different times. After cooling, the solid was washed with deionized water and changed to the protonated form by treatment with HCl solutions of different concentrations

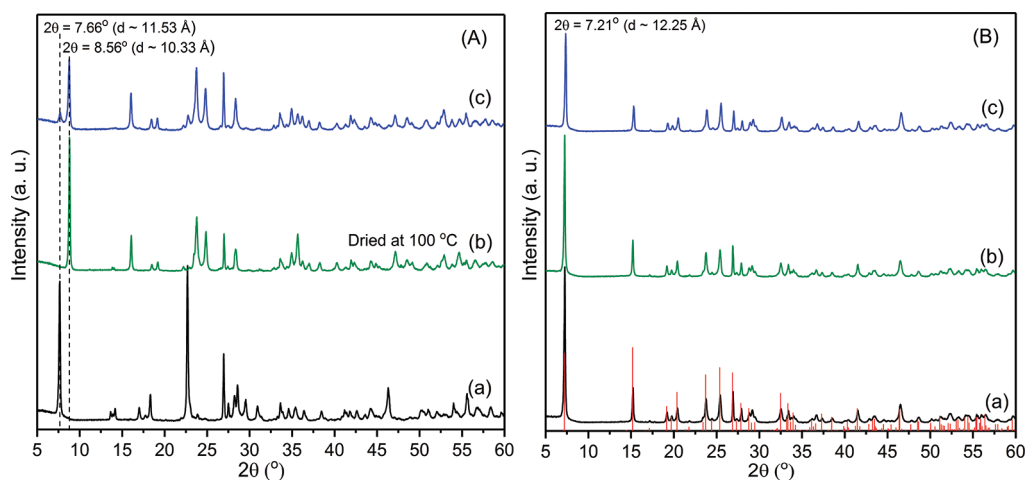


**Figure 2.** (A) XRD patterns of sodium hydrogen zirconium phosphate synthesized using  $\text{ZrOCl}_2 \cdot 8\text{H}_2\text{O} : 4\text{NaH}_2\text{PO}_4 \cdot \text{H}_2\text{O} : 0.3\text{NaF}$  at  $120^\circ\text{C}$  for (a) 24 and (c) 48 h; (B) corresponding  $\gamma$ -ZrP after treatment in 0.5 M HCl. Red lines in B indicate peak positions for  $\gamma$ -ZrP (ICDD 04-011-1172).

(0.5–2 M). About 1 g of the solid was placed in  $50\text{ cm}^3$  of HCl solution and stirred for 6 h at room temperature. The sample was washed with copious amounts of deionized water to remove any remaining HCl and finally dried at  $50^\circ\text{C}$ . Another series of  $\gamma$ -ZrP was prepared using  $\text{NH}_4\text{H}_2\text{PO}_4$  as the phosphate source.

For comparison of ion-exchange properties, gel ZrP was synthesized by precipitation of an aqueous solution of 0.2 M  $\text{ZrOCl}_2 \cdot 8\text{H}_2\text{O}$  ( $30\text{ cm}^3$ ) with an equal volume of 0.5 M  $\text{H}_3\text{PO}_4$  solution under vigorous magnetic stirring at room temperature. After aging at room temperature for 6 h, the resulting gelatinous zirconium phosphate was vacuum filtered and thoroughly washed with 0.1 M  $\text{H}_3\text{PO}_4$  aqueous solution until free of chloride ions.  $\alpha$ -ZrP was prepared using 85%  $\text{H}_3\text{PO}_4$  instead of  $\text{NaH}_2\text{PO}_4$ .<sup>38</sup> The  $\text{ZrOCl}_2 \cdot 8\text{H}_2\text{O}$  and  $\text{H}_3\text{PO}_4$  mixture (1:3 ratio) was heated at  $120^\circ\text{C}$  for 24 h, washed with deionized water and dried at  $50^\circ\text{C}$ .

**2.3. Characterization.** Powder X-ray diffraction (XRD) patterns were measured using a Bruker D8 Advance diffractometer (40 kV, 40 mA) equipped with a copper anode ( $\lambda = 1.5406\text{ \AA}$ ) and a LynxEye XE detector. The  $2\theta$  range was from  $5^\circ$  to  $60^\circ$  with a step size of  $0.02^\circ$  and a dwell time of 0.5 s/step. To minimize preferential orientations, some of the samples were either backloaded and measured in the Bragg–Brentano geometry or filled into 0.3 mm  $\phi$  capillary tubes and measured in the Debye–Scherrer geometry. The sample holder was spun at 30 rpm. Thermogravimetric analysis (TGA) was carried out on a Dupont SDT 2960 analyzer with a heating ramp of  $10^\circ\text{C min}^{-1}$  to  $1000^\circ\text{C}$  under nitrogen flow at  $25\text{ cm}^3\text{ min}^{-1}$ . The morphology was observed by scanning electron microscopy (SEM) using a JEOL JSM-6701F instrument. The sample was coated with platinum prior to observation. Transmission electron microscopy (TEM) and selected area electron diffraction (SAED) were carried out using a JEOL JEM-3010 instrument operated at 300 kV. The sample ( $\sim 10\text{ mg}$ ) was dispersed in isopropanol ( $10\text{ cm}^3$ ) and, after sonication, two drops of the supernatant were placed onto a carbon-coated copper grid and dried overnight at room temperature.

**2.4. Ion-Exchange Properties.** The following experiments were conducted: (a) relative affinity of  $\gamma$ - and  $\alpha$ -ZrP for alkali and alkaline-earth metal ions (b) uptake of  $\text{Cs}^+$  from 0.1 to 10 mM, in the pure solution and in the presence of 0.1 M NaCl and 0.05 M  $\text{CaCl}_2$  (c) uptake of 1 mM  $\text{Cs}^+$  as a function of pH and (d) uptake of  $\text{K}^+$  and  $\text{NH}_4^+$  ions from 0.1 to 20 mM. For (a), three solutions containing (i)  $\text{Na}^+$ ,  $\text{K}^+$ ,  $\text{Cs}^+$  (ii)  $\text{Mg}^{2+}$ ,  $\text{Ca}^{2+}$ ,  $\text{Sr}^{2+}$  and (iii)  $\text{Cs}^+$ ,  $\text{Sr}^{2+}$  with each ion concentration at 1 mM were prepared. For (c), the pH of the solution was adjusted to the desired value by addition of HCl solution.

About 20 mg (100 mg for  $\text{K}^+$  and  $\text{NH}_4^+$  uptake) of the material were dispersed into  $25\text{ cm}^3$  of the mixed ion solution and gently stirred at room temperature for 20 h. The concentration of the ions in the solution was measured by ion chromatography using a Dionex ICS-1100 equipped with a CS12A-4 mm column. The amount of ions

adsorbed onto the zirconium phosphate was calculated from the concentration difference in the solution before and after the ion exchange.

The removal efficiency ( $R$ ) of a given cation was calculated according to

$$R(\%) = \frac{C_i - C_e}{C_i} 100\% \quad (1)$$

where  $C_i$  is the initial concentration and  $C_e$  is the equilibrium concentration. The distribution coefficient ( $K_d$ ) was also determined. It is defined as the ratio of the concentration of ions adsorbed per gram of sorbent to the concentration of ions in one  $\text{cm}^3$  of solution, and expressed mathematically as<sup>39</sup>

$$K_d \left( \frac{\text{cm}^3}{\text{g}} \right) = \frac{C_i - C_e}{C_e} \frac{V}{m} \quad (2)$$

where  $V$  is the volume of solution and  $m$  is the mass of sorbent.

### 3. RESULTS AND DISCUSSION

**3.1. Synthesis Using  $\text{NaH}_2\text{PO}_4 \cdot \text{H}_2\text{O}$ .** Sodium dihydrogen phosphate was used as the phosphate source in the synthesis of  $\gamma$ -ZrP. The synthesis gel consisted of  $\text{ZrOCl}_2 \cdot 8\text{H}_2\text{O}$ ,  $\text{NaH}_2\text{PO}_4 \cdot \text{H}_2\text{O}$  and NaF. The molar ratio of  $\text{ZrOCl}_2 \cdot 8\text{H}_2\text{O} : \text{NaH}_2\text{PO}_4 \cdot \text{H}_2\text{O}$  was varied from 1:2 to 1:5, keeping NaF/Zr at 0.3. The product formed with a stoichiometric molar ratio of 1:2 for  $\text{ZrOCl}_2 \cdot 8\text{H}_2\text{O} : \text{NaH}_2\text{PO}_4 \cdot \text{H}_2\text{O}$  was of low crystallinity. Hence higher ratios were used. The X-ray diffractograms of the solids obtained using a molar ratio of 1:4 (Figure 1) and 1:5 (Figure S2A) showed several sharp peaks. Based on the database, hydrated sodium zirconium hydrogen phosphates with different water content were formed (Figure S1). These were identified as  $\text{NaHZr}(\text{PO}_4)_2 \cdot x\text{H}_2\text{O}$  (ICDD 00-033-1311) and  $\text{NaHZr}(\text{PO}_4)_2 \cdot 2.5\text{H}_2\text{O}$  (ICDD 00-032-1217). Half sodium-exchanged forms of  $\gamma$ -zirconium phosphate have been reported previously.<sup>35,36</sup> The peaks at  $2\theta \approx 7.66^\circ$  ( $d \approx 11.5\text{ \AA}$ ) and  $8.56^\circ$  ( $d \approx 10.3\text{ \AA}$ ) correspond to the basal spacing (Figure 2A). Samples dried at  $50^\circ\text{C}$  may show only one peak at  $2\theta \approx 7.66^\circ$  or both peaks. Their relative intensity varied depending on the state of hydration. For instance, after drying at  $100^\circ\text{C}$  for 5 h, the peak at  $2\theta \approx 7.66^\circ$  was no longer visible, and only that at  $2\theta \approx 8.56^\circ$  could be seen (Figure 2A(b)). The desorption of water from the layered structure leads to a smaller basal spacing.

Regardless of the state of hydration of the sodium zirconium hydrogen phosphate, ion exchange with dilute HCl easily forms

$\gamma$ -ZrP. A simple treatment with 0.5 M HCl for 6 h was sufficient to form pure phase  $\gamma$ -ZrP. The XRD pattern agrees well with that in the PDF database for  $\text{Zr}(\text{PO}_4)(\text{H}_2\text{PO}_4)\cdot 2\text{H}_2\text{O}$  (ICDD 04–011–1172). The first reflection at  $2\theta \approx 7.21^\circ$  corresponds to the basal distance of 12.25 Å (Figure 1B).

As expected from formula, two moles of water were lost per mole of  $\gamma$ -ZrP when the sample was heated under nitrogen flow during thermogravimetric analysis (Figure 3). The loss from

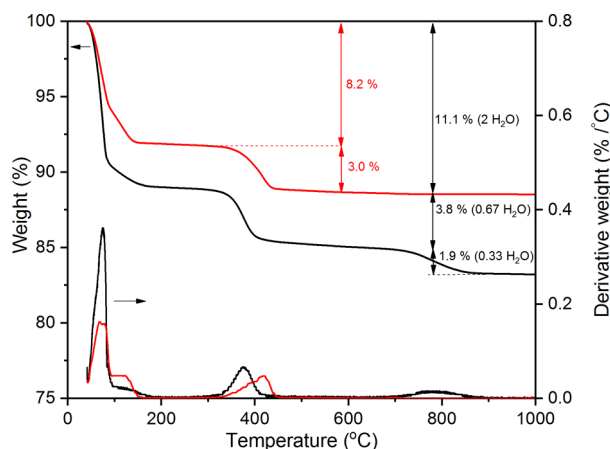


**Figure 3.** TGA curves of  $\gamma$ -NaZrP (red lines: sample a in Figure 2A) and corresponding  $\gamma$ -ZrP (black lines).

the interlayer space occurs below 160 °C and is associated with the formation of anhydrous  $\beta$ -ZrP which can easily revert back to the  $\gamma$ -form under 90% relative humidity at room temperature.<sup>30</sup> A further weight loss occurred at higher temperatures. About 0.67 and 0.33 mol of water were lost per formula unit from 340–420 °C and from 700–860 °C, respectively. This evolution of water has been attributed to condensation of hydroxyls to form a layered  $\gamma$ -zirconium pyrophosphate followed by its transformation to the cubic form.<sup>30,40</sup> In comparison, a typical thermogram for sodium zirconium hydrogen phosphate shows a two- rather than a three-step weight loss (Figure 3). Below 160 °C, removal of water from the interlayer space gives rise to the first weight loss of 8.2%. From the slope of the TGA curve, the initial rate of water loss was high but decreased above  $\sim 100$  °C as more strongly hydrogen-bonded water molecules were lost. This agrees with the XRD results showing a decrease in the  $d_{(001)}$  basal distance after drying at 100 °C. The water content in the sodium zirconium hydrogen phosphate sample is estimated to be  $\sim 1.5$  mol, which is variable depending on the state of drying. From  $\sim 350$ – $450$  °C, structural reorganization results in a smaller second weight loss, 3.0%. XRD of the sample after calcination at 500 °C for 5 h shows that  $\text{NaZr}_2(\text{PO}_4)_3$ ,  $\text{ZrP}_2\text{O}_7$ , and  $\text{NaPO}_3$  were formed (Figure S3).

Scanning electron micrographs revealed that the sodium zirconium hydrogen phosphate formed rather regular micron-sized platelets. The morphology was squarish to tetragonal with thickness of  $\sim 50$ – $60$  nm (Figure 4a). No obvious change in the morphology or size of the platelets was observed after the HCl treatment to form  $\gamma$ -ZrP (Figure 4b). The morphology was similar for  $\gamma$ -ZrP formed using P/Zr ratio of 5 although the platelets were slightly thicker,  $\sim 70$  nm (Figure S4). Although NaF and HCl were successively used during the synthesis, no signals of these elements were detected by energy dispersive X-ray spectroscopy, attesting to the purity of the samples (Figure

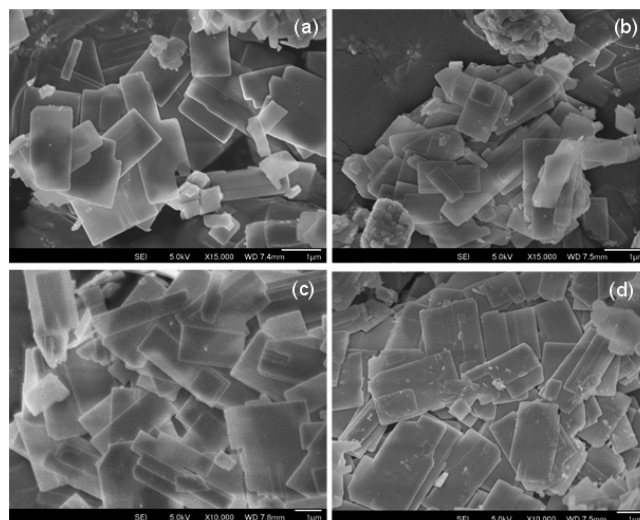


**Figure 4.** Scanning electron micrographs of (a, c) sodium zirconium phosphate and corresponding (b, d)  $\gamma$ -ZrP synthesized for (a, b) 24 and (c, d) 48 h at 120 °C.

S5). Extending the synthesis time from 24 to 48 h resulted in slightly bigger platelets (Figure 4c, d). Transmission electron microscopy also corroborated the tetragonal morphology of  $\gamma$ -ZrP (Figure 5a). The selected area electron diffraction (SAED) indexing confirmed that the crystal growth proceeded along the a and b directions (Figure 5b).

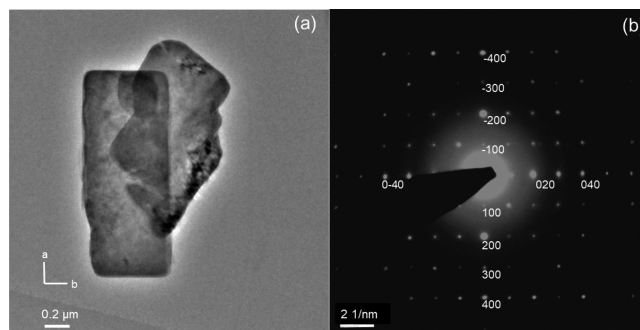


**Figure 5.** (a) TEM image and (b) SAED of  $\gamma$ -ZrP crystal lying flat on Cu grid.

The synthesis of sodium zirconium hydrogen phosphate was also investigated in the absence of the fluoride mineralizer. A longer heating time of 3 days (instead of 1 day) at 120 °C was required. The XRD peaks were broader, indicating that the crystallites were smaller and of lower crystallinity (Figure 6). This agrees well with the scanning electron micrographs of  $\gamma$ -ZrP nanoplatelets, which were smaller and more irregular in shape.

**3.2. Synthesis Using  $\text{NH}_4\text{H}_2\text{PO}_4$ .** Besides  $\text{NaH}_2\text{PO}_4\cdot\text{H}_2\text{O}$ , dihydrogen ammonium phosphate,  $\text{NH}_4\text{H}_2\text{PO}_4$ , was investigated for the synthesis of  $\gamma$ -ZrP. Whereas with the sodium salt, a molar ratio of 4 was required, a molar ratio of P/Zr of 3 was sufficient with the ammonium phosphate to form compounds of high crystallinity. The X-ray diffractogram of the as-synthesized material confirmed that monoammonium  $\gamma$ -zirconium phosphate,  $\gamma\text{-Zr}(\text{PO}_4)(\text{NH}_4\text{HPO}_4)$ , was formed (ICDD 04–014–2214). The first peak at  $2\theta \approx 7.85^\circ$  corresponds to a basal spacing of 11.25 Å, which is slightly smaller than the basal spacing of 11.53 Å observed for the

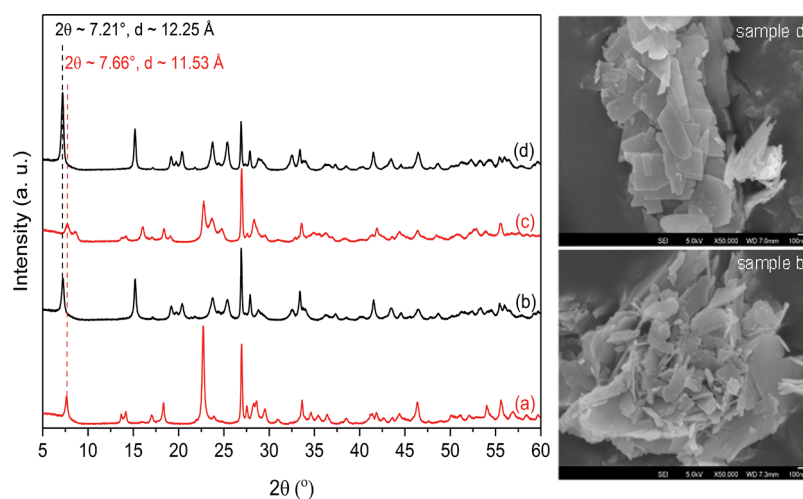


**Figure 6.** XRD and SEM of materials synthesized without NaF at  $\text{NaH}_2\text{PO}_4 \cdot \text{H}_2\text{O}/\text{ZrOCl}_2 \cdot 8\text{H}_2\text{O}$  ratio of (a) 4 and (c) 5; (b, d) after treatment in 0.5 M HCl.

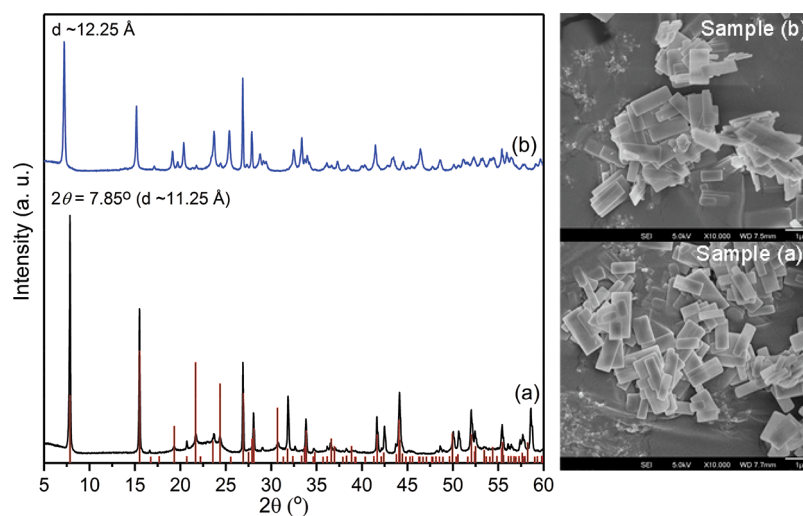


**Figure 7.** XRD and SEM of (a)  $\gamma\text{-Zr}(\text{PO}_4)(\text{NH}_4\text{HPO}_4)$  synthesized using  $\text{ZrOCl}_2 \cdot 8\text{H}_2\text{O} : 3\text{NH}_4\text{H}_2\text{PO}_4 : 0.3\text{NaF}$  and (b) after ion exchanging with 2 M HCl solution; red lines, fitting with database (ICDD 04–014–2214).

sodium zirconium hydrogen phosphate (Figure 7). The ammonium ions in  $\gamma\text{-Zr}(\text{PO}_4)(\text{NH}_4\text{HPO}_4)$  can undergo hydrogen bonding with the neighboring oxygens. This can lower the free energy of formation so that a smaller P/Zr ratio is sufficient, compared to that required for the synthesis of the sodium product.<sup>29</sup>

To form dihydrogen  $\gamma\text{-ZrP}$ , the concentration of the acid is important. A minimum of 2 M HCl is necessary as lower acid concentrations of 0.5–1 M led to incomplete transformation. This could be due to hydrogen bonded ammonium ion, making it more difficult to exchange with the proton.<sup>29</sup> The SEM showed that monoammonium  $\gamma$ -zirconium phosphate also formed rectangular platelets of micron-size, similar to the sodium zirconium hydrogen phosphate. Again, the morphology was retained after ion-exchange with HCl to yield  $\gamma\text{-ZrP}$ .

**3.3. Ion-Exchange Properties.** The uptake of selected ions by crystalline  $\gamma\text{-ZrP}$  was investigated. Cesium-selective sorbents are of interest as cesium is a major nuclear fission product found in circulating water of nuclear reactors. A number of materials have been investigated for this purpose, including potassium cobalt hexacyanoferrate, zeolites, crystalline silicotitanates, biotite micas, pharmacosiderites, and

phlogopites. However, in all cases, the distribution coefficients decreased substantially for cesium concentration above 1  $\mu\text{M}$ .<sup>41–43</sup> Furthermore, some of these materials, e.g., the metal ferrocyanides, suffer from slow kinetics and instability below pH 2.<sup>44</sup>  $\gamma\text{-ZrP}$  was previously reported to show high selectivity to  $\text{Cs}^+$  in the presence of other ions like  $\text{Na}^+$ ,  $\text{Ca}^{2+}$ , and  $\text{Sr}^{2+}$ .<sup>45</sup> However, no details of the crystalline state was given. Therefore, it is of interest to study the ion exchange properties of the highly crystalline  $\gamma\text{-ZrP}$  synthesized by the present method. A comparison is made with crystalline  $\alpha\text{-ZrP}$  formed by the same method (XRD and SEM in Figure S6).

Table 2 shows the removal efficiency ( $R$ ) and distribution coefficient ( $K_d$ ) for alkali and alkaline earth ions in mixed solutions. The removal efficiency for an ion is calculated from the difference in its initial (1 mM in 25  $\text{cm}^3$ ) and final concentration after equilibration with 20 mg ZrP as ion-exchanger/sorbent. The selective pickup of a particular ion is reflected in a high  $K_d$  value. Both  $\alpha\text{-ZrP}$  and  $\gamma\text{-ZrP}$  show the same uptake sequence. For solution 1, the order was  $\text{Cs}^+ > \text{K}^+ > \text{Na}^+$ ; for solution 2,  $\text{Ca}^{2+} \approx \text{Sr}^{2+} > \text{Mg}^{2+}$  and for solution 3,  $\text{Cs}^+ > \text{Sr}^{2+}$ . With the exception of  $\text{Cs}^+$  which is unhydrated, this order follows the trend of the hydrated ionic radii (Table S1).<sup>46</sup>

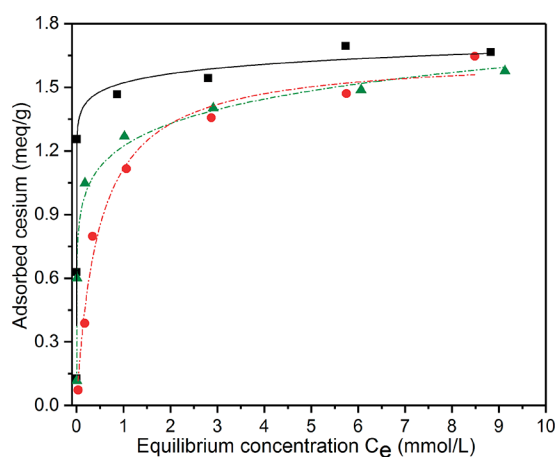
**Table 2. Removal Efficiency (*R*) and Distribution Constant (*K<sub>d</sub>*) of  $\alpha$ -ZrP and  $\gamma$ -ZrP**

solution	cations	<i>R</i> (%)		<i>K<sub>d</sub></i> (cm <sup>3</sup> /g)	
		$\gamma$ -ZrP	$\alpha$ -ZrP	$\gamma$ -ZrP	$\alpha$ -ZrP
1	Na <sup>+</sup>	3.03	2.56	39	33
	K <sup>+</sup>	12.7	3.63	182	47
	Cs <sup>+</sup>	97.3	9.27	49400	128
2	Mg <sup>2+</sup>	3.04	1.11	39	14
	Ca <sup>2+</sup>	27.9	6.96	483	94
	Sr <sup>2+</sup>	26.4	5.70	450	76
3	Cs <sup>+</sup>	94.7	5.82	22400	77
	Sr <sup>2+</sup>	15.1	3.37	223	44

The larger the size of the hydrated ion, the lower the adsorption.<sup>47</sup> A striking feature of  $\gamma$ -ZrP is its very pronounced selectivity to Cs<sup>+</sup>. In the presence of Na<sup>+</sup> and K<sup>+</sup>, the Cs<sup>+</sup> removal efficiency, *R*, was 97.3% with an extremely high distribution coefficient, *K<sub>d</sub>*, of 49 400 cm<sup>3</sup>/g.

$\gamma$ -ZrP has a much higher uptake capacity than  $\alpha$ -ZrP for all ions investigated, although the latter has smaller crystallites (Figure S6b) and a larger surface area (33 vs 6.7 m<sup>2</sup>/g). Hence, the higher uptake by  $\gamma$ -ZrP has to be attributed to other factors, in particular, the presence of dihydrogen phosphate and the larger interlayer distance. The dissociation constant at 25 °C for H<sub>2</sub>PO<sub>4</sub><sup>-</sup> is 6.31 × 10<sup>-8</sup>, which is much larger than 4.22 × 10<sup>-13</sup> for HPO<sub>4</sub><sup>2-</sup>.<sup>48</sup> Therefore, the proton in H<sub>2</sub>PO<sub>4</sub><sup>-</sup> should be much more readily exchangeable with other ions. In contrast,  $\alpha$ -ZrP does not contain dihydrogen phosphate groups but rather HPO<sub>4</sub><sup>2-</sup>, resulting in a much lower ion exchange.

The adsorption isotherm of Cs<sup>+</sup> at pH 5.5 was determined for  $\gamma$ -ZrP (Figure 8). The high uptake at low Cs<sup>+</sup> concentration

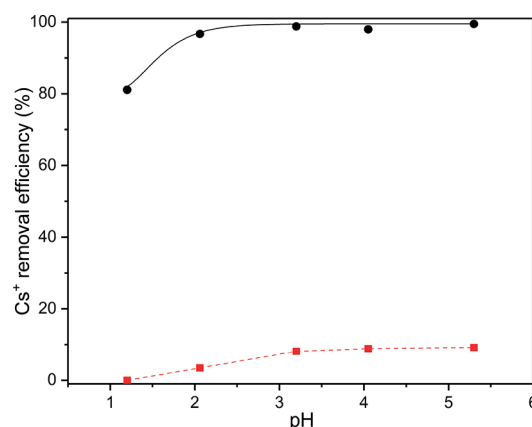
**Figure 8.** Adsorption isotherms of Cs<sup>+</sup> on  $\gamma$ -ZrP (■) in aqueous CsCl solutions (pH 5.5), (●) in the presence of 0.1 M NaCl (pH 5.5), (▲) in the presence of 0.05 M CaCl<sub>2</sub> (pH 5.1).

indicates a very strong interaction between Cs<sup>+</sup> and  $\gamma$ -ZrP. Such an adsorption isotherm can be classified as a *H*-type (high affinity).<sup>49</sup> For Cs<sup>+</sup> concentration >1.5 mmol/L, the uptake increased very gradually to 1.69 mequiv/g. This is somewhat larger than the value of 1.35 mequiv/g reported previously for  $\gamma$ -ZrP.<sup>45</sup> However, as  $\gamma$ -ZrP has a theoretical exchange capacity of 6.27 mequiv/g, the uptake involved about 27% of the exchangeable protons. Hence, slightly more than 50% of the protons from the first ionization of H<sub>2</sub>PO<sub>4</sub><sup>-</sup> are exchanged. Even at this level, the practical exchange capacity of  $\gamma$ -ZrP is

substantially higher than the total exchange capacity of smectites (0.8–1.2 mequiv/g) and some zeolites.<sup>50,51</sup>

In the presence of 10–1000 molar excess of Na<sup>+</sup> and Ca<sup>2+</sup>, the adsorption of Cs<sup>+</sup> was only slightly reduced despite the much higher concentration of the competing ions (Figure 8). The presence of Ca<sup>2+</sup> has a smaller effect on Cs<sup>+</sup> adsorption than the Na<sup>+</sup>. This is likely due to a more hindered access to the interlayer space for the larger hydrated Ca<sup>2+</sup> ion (4.12 Å) as compared to the smaller Na<sup>+</sup> (3.58 Å). Moreover, at the highest equilibrium concentration of ~9 mM Cs<sup>+</sup>, the adsorbed amount was very close to that without the added ions. In contrast,  $\alpha$ -ZrP shows much lower uptake of Cs<sup>+</sup>, with only ~0.32 mequiv/g vs 1.69 mequiv/g for  $\gamma$ -ZrP at ~9 mM Cs<sup>+</sup> concentration (Figure S7). In the presence of competing ions like Ca<sup>2+</sup>, its adsorption was further decreased.

A unique feature of  $\gamma$ -ZrP is the stability under acidic conditions. The uptake of Cs<sup>+</sup> was investigated in the pH range of 1.2 to 5.5 (Figure 9). The removal efficiency by  $\gamma$ -ZrP was

**Figure 9.** Removal efficiency of cesium by (■)  $\alpha$ -ZrP and (●)  $\gamma$ -ZrP versus pH.

>98% for pH > 2 and decreased to 81% for pH 1.2. This can be attributed to the high H<sup>+</sup> concentration which competes with Cs<sup>+</sup> so that at very low pH, the ion exchange equilibrium H<sup>+</sup> ⇌ Cs<sup>+</sup> will be in favor of the protonated  $\gamma$ -ZrP. The Cs<sup>+</sup> removal efficiency by  $\alpha$ -ZrP was much poorer, with <10% for pH > 3 and falling to almost zero at pH 1.2.

Besides its cation exchange property, zirconium phosphate also has the advantage of being biocompatible because of the low toxicity of zirconium.<sup>52</sup> Zirconium phosphate is used in sorbent cartridges to purify the spent dialysate from renal treatment.<sup>53,54</sup> Such sorbent cartridges are an important component of wearable and portable dialysis devices that allow renal patients to have more flexibility in their lifestyle and have better health outcomes due to the continuous removal of wastes from the body.<sup>55</sup> Currently, amorphous zirconium phosphate gel is loaded in these sorbent systems. We evaluated the sorption capacity of the crystalline  $\gamma$ -ZrP and the amorphous gel ZrP for NH<sub>4</sub><sup>+</sup> and K<sup>+</sup>, two cations typically found in the spent dialysate. At low concentrations, both gel and  $\gamma$ -ZrP show similar uptake of these ions (Figure 10). However, above 0.5 mmol/L, the uptake of K<sup>+</sup> and NH<sub>4</sub><sup>+</sup> was significantly higher for  $\gamma$ -ZrP than the gel. These results clearly show the benefits of having high crystalline zirconium phosphate with uniform cavities as compared to a range of cavity sizes in the amorphous gel. Hence, at the same removal

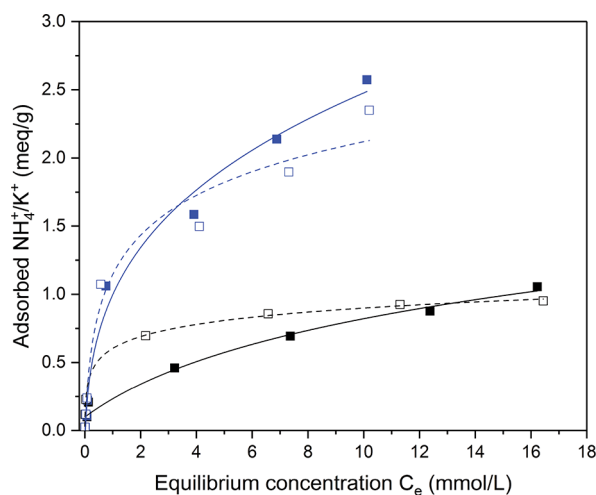


**Figure 10.** Uptake by  $\gamma$ -ZrP (blue) and gel ZrP (black) for  $\text{NH}_4^+$  (■) and  $\text{K}^+$  (□).

capacity, smaller amounts of the zirconium phosphate can be used, translating into lighter and more portable cartridges.

#### 4. CONCLUSIONS

Highly crystalline  $\gamma$ -ZrP was synthesized via a liquid-assisted mechanochemistry-based route. In contrast to existing protocols that require a large excess of the phosphate source, molar P/Zr ratios of 3–5 are sufficient with the new method. The only solvent in the synthesis originated from the water of crystallization present in the reactants. The addition of a small amount of sodium fluoride as a mineralizer increased the crystallinity of the  $\gamma$ -ZrP which formed micron-sized platelets with square to rectangular shape. The crystalline  $\gamma$ -ZrP selectively adsorbs  $\text{Cs}^+$  with removal efficiencies >98% even in the presence of a 1000- or 500-fold excess of  $\text{Na}^+$  or  $\text{Ca}^{2+}$  ions, respectively. The high selectivity and uptake of  $\text{Cs}^+$  is maintained under acidic conditions, making  $\gamma$ -ZrP a very useful ion exchanger. The crystalline  $\gamma$ -ZrP also shows excellent adsorption for  $\text{NH}_4^+$  and  $\text{K}^+$  with much higher binding capacity than the gel ZrP, offering the possibility to reduce the size of sorbent dialyzer cartridges.

#### ■ ASSOCIATED CONTENT

##### Supporting Information

The Supporting Information is available free of charge on the ACS Publications website at DOI: 10.1021/acs.inorgchem.7b03202.

XRD and SEM of samples synthesized at different ratios of  $\text{NaH}_2\text{PO}_4/\text{Zr}$ ; XRD of 500 °C-calcined sodium zirconium phosphate; XRD and SEM of  $\alpha$ -ZrP, elemental analysis by EDS, and adsorption isotherms of cesium on  $\alpha$ -ZrP (PDF)

#### ■ AUTHOR INFORMATION

##### Corresponding Author

\*E-mail: chmcgk@nus.edu.sg

##### ORCID

Gaik-Khuan Chuah: 0000-0002-4739-9405

##### Author Contributions

The manuscript was written through contributions of all authors.

#### Notes

The authors declare no competing financial interest.

#### ■ ACKNOWLEDGMENTS

Financial support from the Academic Research Grant, R-143-000-667-114, National University of Singapore, is gratefully acknowledged. Y.C. thanks NUS-IPP program for award of a research scholarship.

#### ■ REFERENCES

- (1) Clearfield, A. Inorganic Ion Exchangers, Past, Present, and Future. *Solvent Extr. Ion Exch.* **2000**, *18*, 655–678.
- (2) Clearfield, A. Role of Ion Exchange in Solid-State Chemistry. *Chem. Rev.* **1988**, *88*, 125–148.
- (3) Alberti, G.; Cardini-Galli, P.; Costantino, U.; Torracca, E. Crystalline Insoluble Salts of Polybasic Metals—I Ion-Exchange Properties of Crystalline Titanium Phosphate. *J. Inorg. Nucl. Chem.* **1967**, *29*, 571–578.
- (4) Clearfield, A.; Thakur, D. S. Zirconium and Titanium Phosphates as Catalysts: A Review. *Appl. Catal.* **1986**, *26*, 1–26.
- (5) Segawa, K.; Kurusu, Y.; Nakajima, Y.; Kinoshita, M. Characterization of Crystalline Zirconium Phosphates and Their Isomerization Activities. *J. Catal.* **1985**, *94*, 491–500.
- (6) Sinhamahapatra, A.; Sutradhar, N.; Roy, B.; Tarafdar, A.; Bajaj, H. C.; Panda, A. B. Mesoporous Zirconium Phosphate Catalyzed Reactions: Synthesis of Industrially Important Chemicals in Solvent-Free Conditions. *Appl. Catal., A* **2010**, *385*, 22–30.
- (7) Pica, M.; Nocchetti, M.; Ridolfi, B.; Donnadio, A.; Costantino, F.; Gentili, P. L.; Casciola, M. Nanosized Zirconium Phosphate/AgCl Composite Materials: A New Synergy for Efficient Photocatalytic Degradation of Organic Dye Pollutants. *J. Mater. Chem. A* **2015**, *3*, 5525–5534.
- (8) Li, D.; Zhang, Y.; Zhou, B. pH-Responsive Drug Delivery System Based on AIE Luminogen Functionalized Layered Zirconium Phosphate Nano-Platelets. *J. Solid State Chem.* **2015**, *225*, 427–430.
- (9) Saxena, V.; Diaz, A.; Clearfield, A.; Batteas, J. D.; Hussain, M. D. Zirconium Phosphate Nanoplatelets: A Biocompatible Nanomaterial for Drug Delivery to Cancer. *Nanoscale* **2013**, *5*, 2328–2336.
- (10) Díaz, A.; Saxena, V.; González, J.; David, A.; Casañas, B.; Carpenter, C.; Batteas, J. D.; Colón, J. L.; Clearfield, A.; Delwar Hussain, M. Zirconium Phosphate Nano-Platelets: A Novel Platform for Drug Delivery in Cancer Therapy. *Chem. Commun.* **2012**, *48*, 1754–1756.
- (11) Casciola, M.; Bagnasco, G.; Donnadio, A.; Micoli, L.; Pica, M.; Sganappa, M.; Turco, M. Conductivity and Methanol Permeability of Nafion-Zirconium Phosphate Composite Membranes Containing High Aspect Ratio Filler Particles. *Fuel Cells* **2009**, *9*, 394–400.
- (12) Casciola, M.; Capitani, D.; Comite, A.; Donnadio, A.; Frittella, V.; Pica, M.; Sganappa, M.; Varzi, A. Nafion-Zirconium Phosphate Nanocomposite Membranes with High Filler Loadings: Conductivity and Mechanical Properties. *Fuel Cells* **2008**, *8*, 217–224.
- (13) Alberti, G.; Casciola, M.; Pica, M.; Di Cesare, G. Preparation of Nano-Structured Polymeric Proton Conducting Membranes for Use in Fuel Cells. *Ann. N. Y. Acad. Sci.* **2003**, *984*, 208–225.
- (14) Sun, L.; Boo, W. J.; Sun, D.; Clearfield, A.; Sue, H.-J. Preparation of Exfoliated Epoxy/ $\alpha$ -Zirconium Phosphate Nanocomposites Containing High Aspect Ratio Nanoplatelets. *Chem. Mater.* **2007**, *19*, 1749–1754.
- (15) Casciola, M.; Alberti, G.; Donnadio, A.; Pica, M.; Marmottini, F.; Bottino, A.; Piaggio, P. Gels of Zirconium Phosphate in Organic Solvents and Their Use for the Preparation of Polymeric Nanocomposites. *J. Mater. Chem.* **2005**, *15*, 4262–4267.
- (16) Wong, M.; Ishige, R.; White, K. L.; Li, P.; Kim, D.; Krishnamoorti, R.; Gunther, R.; Higuchi, T.; Jinnai, H.; Takahara, A.; et al. Large-Scale Self-Assembled Zirconium Phosphate Smectic Layers Via a Simple Spray-Coating Process. *Nat. Commun.* **2014**, *5*, 3589.

- (17) Brunet, E.; Alhendawi, H. M.; Cerro, C.; de la Mata, M. J.; Juanes, O.; Rodríguez-Ubis, J. C. Hydrogen Storage in a Highly Porous Solid Derived from  $\gamma$ -Zirconium Phosphate. *Angew. Chem., Int. Ed.* **2006**, *45*, 6918–6920.
- (18) Agar, J. W. Review: Understanding Sorbent Dialysis Systems. *Nephrology* **2010**, *15*, 406–411.
- (19) Clearfield, A.; Stynes, J. The Preparation of Crystalline Zirconium Phosphate and Some Observations on Its Ion Exchange Behaviour. *J. Inorg. Nucl. Chem.* **1964**, *26*, 117–129.
- (20) Clearfield, A.; Smith, G. D. Crystallography and Structure of  $\alpha$ -Zirconium Bis(Monohydrogen Orthophosphate) Monohydrate. *Inorg. Chem.* **1969**, *8*, 431–436.
- (21) Kijima, T. Direct Preparation of Theta-Zirconium Phosphate. *Bull. Chem. Soc. Jpn.* **1982**, *55*, 3031–3032.
- (22) Clearfield, A.; Blessing, R. H.; Stynes, J. A. New Crystalline Phases of Zirconium Phosphate Possessing Ion-Exchange Properties. *J. Inorg. Nucl. Chem.* **1968**, *30*, 2249–2258.
- (23) Poojary, D. M.; Shpeizer, B.; Clearfield, A. X-Ray Powder Structure and Rietveld Refinement of  $\gamma$ -Zirconium Phosphate,  $Zr(PO_4)(H_2PO_4) \cdot 2H_2O$ . *J. Chem. Soc., Dalton Trans.* **1995**, 111–113.
- (24) Krogh Andersen, A. M.; Norby, P.; Hanson, J. C.; Vogt, T. Preparation and Characterization of a New 3-Dimensional Zirconium Hydrogen Phosphate,  $\tau$ - $Zr(HPO_4)_2$ . Determination of the Complete Crystal Structure Combining Synchrotron X-Ray Single-Crystal Diffraction and Neutron Powder Diffraction. *Inorg. Chem.* **1998**, *37*, 876–881.
- (25) Clearfield, A. Inorganic Ion Exchangers with Layered Structures. *Annu. Rev. Mater. Sci.* **1984**, *14*, 205–229.
- (26) Clearfield, A.; Duax, W.; Medina, A.; Smith, G. D.; Thomas, J. On the Mechanism of Ion Exchange in Crystalline Zirconium Phosphates. I. Sodium Ion Exchange of  $\alpha$ -Zirconium Phosphate. *J. Phys. Chem.* **1969**, *73*, 3424–3430.
- (27) Albertsson, J.; Oskarsson, A.; Tellgren, R.; Thomas, J. O. Inorganic Ion Exchangers. 10. A Neutron Powder Diffraction Study of the Hydrogen Bond Geometry in  $\alpha$ -Zirconium Bis(Monohydrogen Orthophosphate) Monohydrate. A Model for the Ion Exchange. *J. Phys. Chem.* **1977**, *81*, 1574–1578.
- (28) Clayden, N. J. Solid-State Nuclear Magnetic Resonance Spectroscopic Study of  $\gamma$ -Zirconium Phosphate. *J. Chem. Soc., Dalton Trans.* **1987**, 1877–1881.
- (29) Poojary, D. M.; Zhang, B.; Dong, Y.; Peng, G.; Clearfield, A. X-Ray Powder Structure of Monoammonium-Exchanged Phase of  $\gamma$ -Zirconium Phosphate,  $Zr(PO_4)(NH_4HPO_4)$ . *J. Phys. Chem.* **1994**, *98*, 13616–13620.
- (30) Alberti, G.; Bernasconi, M.; Casciola, M. Preparation of  $\gamma$ -Zirconium Phosphate Microcrystals with High Degree of Crystallinity and Proton Conductivity of Their Hydrogen and Ammonium Forms. *React. Polym.* **1989**, *11*, 245–252.
- (31) Alberti, G.; Brunet, E.; Dionigi, C.; Juanes, O.; de la Mata, M. J.; Rodríguez-Ubis, J. C.; Vivani, R. Shaping Solid-State Supramolecular Cavities: Chemically Induced Accordionlike Movement of  $\gamma$ -Zirconium Phosphate Containing Polyethylenoxide Pillars. *Angew. Chem., Int. Ed.* **1999**, *38*, 3351–3353.
- (32) Costantino, U.; Szirtes, L.; Környei, J. Self-Diffusion of the Sodium Ion in the Monosodium and Disodium Forms of  $\alpha$ - and  $\gamma$ -Zirconium Phosphate. *J. Chromatogr. A* **1980**, *201*, 167–174.
- (33) Alberti, G. Syntheses, Crystalline Structure, and Ion-Exchange Properties of Insoluble Acid Salts of Tetravalent Metals and Their Salt Forms. *Acc. Chem. Res.* **1978**, *11*, 163–170.
- (34) Clearfield, A.; Kalnins, J. M. On the Mechanism of Ion Exchange in Zirconium Phosphates—XXIII Exchange of First Row Divalent Transition Elements on  $\gamma$ -Zirconium Phosphate. *J. Inorg. Nucl. Chem.* **1978**, *40*, 1933–1936.
- (35) Allulli, S.; Ferragina, C.; La Ginestra, A.; Massucci, M.; Tomassini, N. Preparation and Ion-Exchange Properties of a New Phase of the Crystalline Titanium Phosphate,  $Ti(HPO_4)_2 \cdot 2H_2O$ . *J. Inorg. Nucl. Chem.* **1977**, *39*, 1043–1048.
- (36) Yamanaka, S.; Tanaka, M. Formation Region and Structural Model of  $\gamma$ -Zirconium Phosphate. *J. Inorg. Nucl. Chem.* **1979**, *41*, 45–48.
- (37) Kobayashi, E. A Study of Inorganic Ion Exchangers. VII. The Synthesis of  $\gamma$ - $NH_4ZrH(PO_4)_2$  and Ion-Exchange Properties of  $\gamma$ - $Zr(HPO_4)_2 \cdot 2H_2O$ . *Bull. Chem. Soc. Jpn.* **1983**, *56*, 3756–3760.
- (38) Cheng, Y.; Wang, X. T.; Jaenicke, S.; Chuah, G.-K. Minimalistic Liquid-Assisted Route to Highly Crystalline  $\alpha$ -Zirconium Phosphate. *ChemSusChem* **2017**, *10*, 3235–3242.
- (39) Silbernagel, R.; Martin, C. H.; Clearfield, A. Zirconium (IV) Phosphonate-Phosphates as Efficient Ion-Exchange Materials. *Inorg. Chem.* **2016**, *55*, 1651–1656.
- (40) Shakshooki, S.; EL-Tarhuni, S.; EL-Hamady, A. Synthesis and Characterization of Pellicular  $\gamma$ -Zirconium Phosphate Fibrous Cerium Phosphate Nanocomposite Membranes. *Am. J. Chem.* **2014**, *4*, 109–115.
- (41) Brown, G.; Carson, K.; DesChane, J.; Elovich, R. *Performance Evaluation of 24 Ion Exchange Materials for Removing Cesium and Strontium from Actual and Simulated N-Reactor Storage Basin Water*; Report PNNL-11711 UC-2030 ; Pacific Northwest National Laboratory: Richland, WA, 1997.10.2172/555252
- (42) Parajuli, D.; Takahashi, A.; Noguchi, H.; Kitajima, A.; Tanaka, H.; Takasaki, M.; Yoshino, K.; Kawamoto, T. Comparative Study of the Factors Associated with the Application of Metal Hexacyanoferrates for Environmental Cs Decontamination. *Chem. Eng. J.* **2016**, *283*, 1322–1328.
- (43) Mukai, H.; Hirose, A.; Motai, S.; Kikuchi, R.; Tanoi, K.; Nakanishi, T. M.; Yaita, T.; Kogure, T. Cesium Adsorption/Desorption Behavior of Clay Minerals Considering Actual Contamination Conditions in Fukushima. *Sci. Rep.* **2016**, *6*, 21543.
- (44) Tranter, T.; Herbst, R.; Todd, T.; Olson, A.; Eldredge, H. Evaluation of Ammonium Molybdophosphate-Polyacrylonitrile (AMP-PAN) as a Cesium Selective Sorbent for the Removal of  $^{137}Cs$  from Acidic Nuclear Waste Solutions. *Adv. Environ. Res.* **2002**, *6*, 107–121.
- (45) Komarneni, S.; Roy, R. Use of  $\gamma$ -Zirconium Phosphate for Cs Removal from Radioactive Waste. *Nature* **1982**, *299*, 707–708.
- (46) Nightingale, E., Jr. Phenomenological Theory of Ion Solvation. Effective Radii of Hydrated Ions. *J. Phys. Chem.* **1959**, *63*, 1381–1387.
- (47) Clearfield, A.; Garces, J. M. On the Mechanism of Ion Exchange in Zirconium Phosphates—XXIV Exchange of Alkali Metal Ions on  $\gamma$ -Zirconium Phosphate. *J. Inorg. Nucl. Chem.* **1979**, *41*, 879–884.
- (48) Larson, J. W.; Zeeb, K. G.; Hepler, L. G. Heat Capacities and Volumes of Dissociation of Phosphoric Acid (1st, 2nd, and 3rd), Bicarbonate Ion, and Bisulfate Ion in Aqueous Solution. *Can. J. Chem.* **1982**, *60*, 2141–2150.
- (49) Giles, C.; MacEwan, T.; Nakhwa, S.; Smith, D. 786. Studies in Adsorption. Part XI. A System of Classification of Solution Adsorption Isotherms, and Its Use in Diagnosis of Adsorption Mechanisms and in Measurement of Specific Surface Areas of Solids. *J. Chem. Soc.* **1960**, 3973–3993.
- (50) Sylvester, P.; Clearfield, A.; Diaz, R. J. Pillared Montmorillonites: Cesium-Selective Ion-Exchange Materials. *Sep. Sci. Technol.* **1999**, *34*, 2293–2305.
- (51) Bortun, A. I.; Bortun, L. N.; Khainakov, S. A.; Clearfield, A. Ion Exchange Properties of the Sodium Phlogopite and Biotite. *Solvent Extr. Ion Exch.* **1998**, *16*, 1067–1090.
- (52) Lee, D. B.; Roberts, M.; Bluchel, C. G.; Odell, R. A. Zirconium: Biomedical and Nephrological Applications. *ASAIO J.* **2010**, *56*, 550–556.
- (53) Wester, M.; Simonis, F.; Gerritsen, K. G.; Boer, W. H.; Wodzig, W. K.; Kooman, J. P.; Joles, J. A. A Regenerable Potassium and Phosphate Sorbent System to Enhance Dialysis Efficacy and Device Portability: An in Vitro Study. *Nephrol., Dial., Transplant.* **2013**, *28*, 2364–2371.
- (54) Ash, S. R. Sorbents in Treatment of Uremia: A Short History and a Great Future. *Semin. Dial.* **2009**, *22*, 615–622.

(55) McGill, R. L.; Bakos, J. R.; Ko, T.; Sandroni, S. E.; Marcus, R. J. Sorbent Hemodialysis: Clinical Experience with New Sorbent Cartridges and Hemodialyzers. *ASAIO J.* **2008**, *54*, 618–621.